Article:
Yang, H, Yao, G and Wen, D (2021) Efficient mixing enhancement by orthogonal injection of shear-thinning fluids in a micro serpentine channel at low Reynolds numbers. Chemical Engineering Science, 235. 116368. ISSN: 0009-2509

https://doi.org/10.1016/j.ces.2020.116368

Efficient Mixing Enhancement by Orthogonal Injection of Shear-Thinning Fluids in a Micro Serpentine Channel at Low Reynolds Numbers

Haie Yang[1], Guice Yao[1 *], Dongsheng Wen[1, 2 *]

1 Beihang University, Beijing, 100191, China

2 University of Leeds, Leeds LS2 9JT, UK

Abstract

Viscoelastic fluids have been recently proposed to promote mixing effect in microfluidic systems, where limited success has been obtained. However, the flow and mixing mechanism of a viscoelastic fluid is still poorly understood, particularly regarding the roles of injection on mixing at low Reynolds numbers. In this work, an efficient mixer by orthogonal injection into a primary flow is proposed. The mixing behaviors of shear-thinning fluids in a serpentine channel with an orthogonal injection were investigated experimentally. Dye visualization and concomitant statistical analysis were conducted to quantitatively characterize the mixing performance and to reveal the flow kinematics. Enhanced mixing is achieved just over a short effective mixing length. The probability distribution functions (PDFs) analysis shows that the mixing efficiency, defined by the normalized concentration of dye intensity[1], can be significantly improved from 22% for the Newtonian fluids to 69% and 76% by using a shear-thinning fluid with polymer concentrations of 25 and 50 ppm, respectively. The decay exponents of shear-thinning fluids plateau at -3.4 indicates the occurrence of elastic instability. The relative-change-ratio fluctuations illustrates that the observation area can generate sufficient elastic stress to induce flow instabilities, resulting in effective mixing in the channel.

Keywords: fluid-structure interactions, elastic turbulence, efficient mixing, microfluidics, non-Newtonian fluid dynamics

Introduction. Mixing is an ubiquitous phenomenon in nature and everyday life, and is of high importance to many applications[2] such as process intensification, enhanced oil recovery[3] and various chemical processes (i.e., chemical synthesis and micro/nano-particle production[4,5]) . The mixing in microfluidics[6] , which is essential for any lab-on-a-chip device (i.e., blood and saliva analysis[7] , future drag diagnosis, and blood plasma mixing[8]), is especially challenging. It is widely accepted that the mixing achieved by a chaotic advection has a much higher efficiency than that purely induced by the molecular diffusion. At the macroscale, it is possible and relatively easy to induce hydrodynamic turbulence by directly increasing the Reynolds number, i.e., $Re = \rho V_a L/\eta$, where ρ and η are the fluid density and viscosity, respectively, V_a is the mean velocity, and L is the characteristic length, via increasing the flow velocity. However at the microscale, the Reynolds number becomes very small due to the small value of the characteristic length, where the prevailing flow is in the laminar flow regime, resulting in a molecular diffusion dominated mixing behavior [9,10]. In addition, the increase of the surface-to-volume ratio at the microscale increases the capillary force, which dominates the interaction between the fluid flow and the channel geometry. To enhance mixing efficiency at the microscale, various approaches[9,11] have been proposed by fabricating complicated channel structures or micromixers[12,13] assisted by external drivers. These approaches, however, have not received practical applications as they still cannot successfully break through the limitation of laminar flow nature. An economic and convenient approach of efficient mixing at the microscale beyond the limitation of laminar flow will be of high value.

Although it is difficult to induce turbulence within the flow of Newtonian fluids in micro systems due to the limitation of laminar flow, a turbulent-like phenomenon with remarkable chaotic advection, which is known as elastic turbulence[14–21], does exist in the flow of a polymeric solution. With small amount of high-

molecular-weight polymer addition into a conventional Newtonian fluid, the fluid shows a non-Newtonian behavior that could exhibit both liquid and solid properties. There are two nonlinearities contribute to the flow instability, inertial nonlinearity and elastic nonlinearity, where the latter is ascribed to the polymer interaction with the primary flow[21]. The elastic stress within the fluids would exhibit a remarkable non-linear growth with shear rate with relaxation characteristics. The Weissenberg number, $Wi = \lambda\dot{\gamma}$, analogous to the definition of *Re*, is used to characterize the degree of elastic nonlinearity, where λ is the longest polymer relaxation time and $\dot{\gamma}$ is the shear rate. Therefore, even at low *Re*, the flow could still transfer from a laminar state to a chaotic advection regime when the *Wi* exceeds a critical value, which could benefit the mixing performance.

However, the mechanisms of chaotic advection induced by the elastic instability and elastic turbulence, is still little known, especially during the transition from a stable to a chaotic state. Recently, a few theoretical and numerical investigations of effective enhancement of mixing by elastic instability/turbulence in micro channels have been conducted in various geometries[21–30], including serpentine channels[23,25,26,31] and abrupt contraction micro channels[1,32]. However, in the experiments conducted within serpentine channels, a relatively long mixing path at a moderate flow rate was still observed, which shows limited enhancement in the mixing [26,27]. Short mixing length was observed for flows in an abrupt contraction microchannel, however the channel structure is too complex and fragile for any practical applications. Additionally, the mixing performance is influenced by the injection even in a serpentine channel with a single semi-band, which is named VDP (Viscous Disk Pump) as illustrated in the dye visualization by Ligrani et al.[33,34]. Therefore, there is a strong need to investigate the influence of injection on the mixing performance along a serpentine channel.

In order to show a strong non-Newtonian behavior[35], working fluids with orders of magnitude higher

viscosity than water were used in previous investigations, which brings a heavy penalty in pressure drop, especially for a high-throughput operation[9]. In addition, most of the working fluids used in these investigations are the Boger fluids, which have nearly constant viscosities in a log-log coordinate with low shear-thinning effects[36–39]. Hitherto, the effects of shear-thinning fluids on the introduction of elastic instability and turbulence have not been exploited effectively.

Addressing such limitations, we propose a new approach of enhancing mixing by combining the advantages of serpentine channel and abrupt contraction micro channel, i.e., a simple orthogonal injection into a micro serpentine channel, that results in a very short mixing length. Such an approach is similar to the work of Qin et al.[40] in the straight channel with a set of small cylinders at the entrance section. In this work, we prove experimentally that the orthogonal injection is a good bridge to connect the homogeneity on mixing wanted by the smallest scale fluctuation and the elastic instabilities, which is dominated by the large-scale fluctuations. [41]. Consequently, a rapid mixing is achieved within a shorted mixing path in the serpentine channel. To sufficiently decrease the effects of chemical additions (e.g. salt and antiseptic) on polymer, which is sensitive to salinity[42], aqueous solutions with a small amount of polyacrylamide are chosen as the working fluids. To reduce the influence of polymer additions on the other physical properties except the viscosity, polymeric solutions with extremely low concentration (25 ppm and 50 ppm) are used. The results provide experimental and theoretical proof of effective mixing due to chaotic flow, as shown by dye pattens, power spectra dependence and fluctuation of concentration variations, and derive a new criterion for predicting the onset of elastic instability with the incorporation of the geometry effects and shear-thinning effects.

Methods. In this manuscript, we investigated the flow of shear-thinning fluids with extremely low concentration in a serpentine channel at low Reynolds number *Re* using dye trajectory method and image

processing analysis. Dye trajectory method shows that remarkable bifurcations are generated within the flow of viscoelastic fluids at low Reynolds number, while the flow of Newtonian fluids stays laminar. Systematic image processing analysis based on the coupling of MATLAB and OpenCV was used to capture features of perturbation within the flow. In addition, we study the statistical properties of mixing by quantitatively analyzing the PDF of normalized dye concentrations, the power spectra and the decay exponents scaling of the total normalized concentration in the observed area.

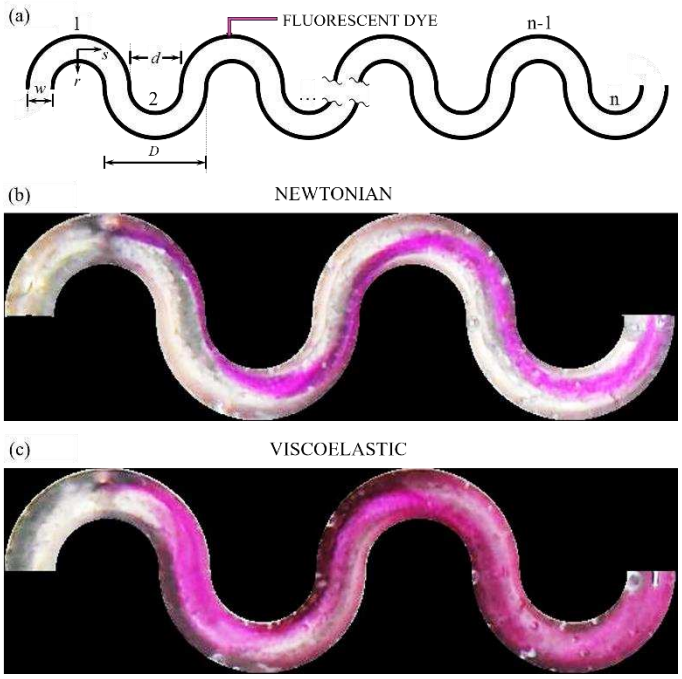

Fig. 1 (a) Schematic of the serpentine channel, showing the injecting point of dye, where n refers to the number of semi C-shaped curved channel, where the definition of C-shaped channel is similar to Ligrani et al. [43], and example dye patterns of (b) Newtonian fluids and (c) shear-thinning fluids with the concentration of 50 ppm, at bulk flowrate of V_b = 3500 μl/min (Wi = 5.89).

Experiments were conducted using a serpentine channel with equal width and depth (W = H = 1mm), fabricated by polyethylene. The schematic view of the test section is shown in Fig.1a. The channel has 20 sections (n = 20). The inner and outer diameters of curvatures are d= 1mm and D= 2mm, respectively. The

dye was injected from the center point of the outer semicircle of the third section in the serpentine channel. A syringe pump (KD Scientific, U.S.A) was used to control the bulk flow rates. The image acquisition system is the same as our previous work[44] and a highspeed camera (I-SPEED 720, U.K.) was used to capture the flow image. The dye was injected by another syringe pump though a syringe needle with a diameter of 0.3mm connected with the serpentine channel. These two syringe pumps are controlled by a synchronizer. The recorded images are digitally transferred (in TIF format) to a personal computer for further analysis (using MATLAB and OpenCV).

The polymeric solution was prepared by adding 25 ppm and 50 ppm of polyacrylamide (PAAM) (M_w=18×10^6 Da) to the deionized water, respectively. For brevity, these two fluids are denoted as 25PAAM and 50PAAM, respectively. No other inorganic salt or sucrose have been added since that the viscosity of dilute polymer has an extremely sensitive reaction to the inorganic such as NaCl[42]. The Newtonian solvent, deionized water, which is denoted as WATER for brevity, has constant viscosity and was used as the base fluid. The Rhodamine B dye was seeded to the corresponding working fluids at a weight ratio of 0.05%. The properties of all working fluids are listed in Table 1. The rheological properties including viscosity and relaxation time of the working fluids were measured by a rheometer (TA Instruments AR100 N, U.S.A) controlled stress rheometer with a stainless-steel plate geometry (40 mm diameter). In this study, the shear viscosity, η, for all the polymer solutions against shear rate is schematically illustrated in Fig. 2. It is shown that the shear viscosity has a significant shear-thinning behavior. The Carreau-Yasuda model was adopted to fit the experimental viscosity as shown by the solid lines. In order to measure the relaxation time, small amplitude oscillatory shear stress (SAOS) tests conducted by the rheometer for the measurements of the storage modulus, G', which represents the energy of elastic storage and the state of the structured materials,

and the loss modulus, G'', which represents viscous dissipation or loss of energy. Frequency sweeps were conducted within linear viscoelastic region when the oscillation shear stress is kept constant at a low value which is 0.01 here. Fig. 3 shows the dependence of polymer relaxation time on the angular frequency from the measurements of SAOS for all the PAAM solutions used in this study. The value of the longest relaxation time, λ, which is estimated in the limit of the angular velocity approaching to zero are summarized in Table 1 for all the non-Newtonian fluids utilized in the study.

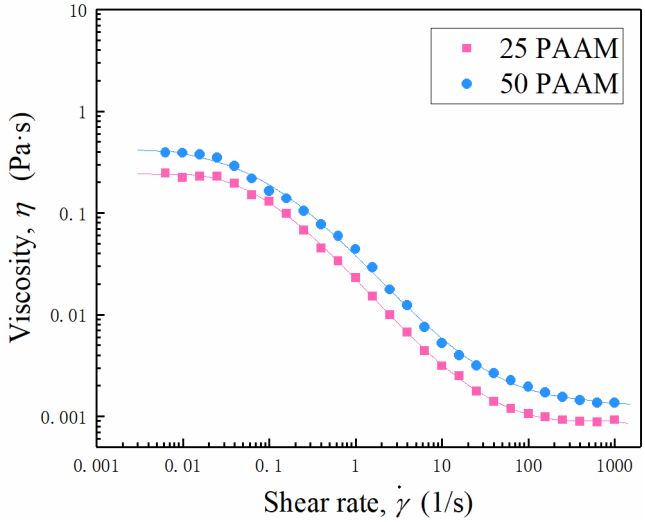

Fig. 2 The viscosity of the shear-thinning fluids versus shear rates, including 25PAAM and 50PAAM.

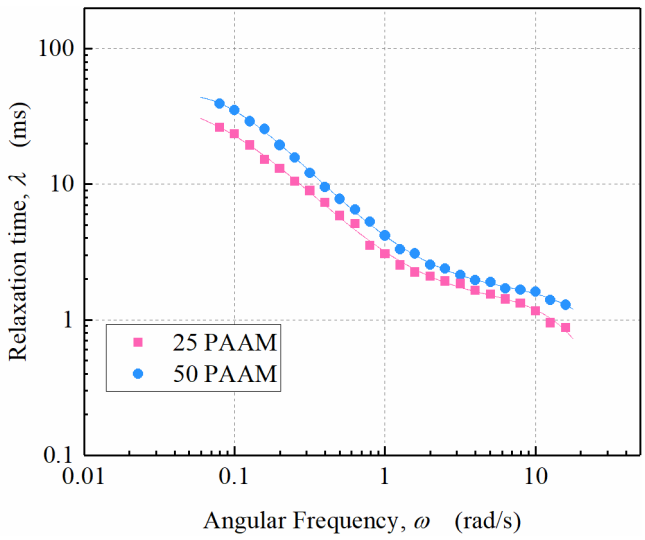

Fig. 3 Relaxation time against the angular frequency obtained from small amplitude oscillatory shear stress measurements for the PAAM solutions with the concentrations of 25 ppm and 50 ppm, respectively.

Throughout the overall study, the Reynolds number is ranging from 0.145 to 0.474, where $Re = \rho UW/\eta$, where U is the bulk flowrate, W is the channel width, η is the viscosity and ρ is the density of the working fluids. The relation of elastic stress and viscous stress is normalized by Weissenberg number, Wi, i.e., $Wi(\dot{\gamma}) = N_1(\dot{\gamma})/2\dot{\gamma}\eta_p(\dot{\gamma})$, where $\dot{\gamma} = U/W$ is the shear rate, N_1 is the first normal stress difference and $\eta_p(\dot{\gamma})$ is the polymeric viscosity which is calculated by $\eta_p = \eta - \eta_s$ [27,45,46]. Wi is ranging from 3.9 to 10.1 in this experiment. With reference to the main stream fluid, the other two dimensionless numbers El and Pe were also estimated. The Elastic number El and the Peclet number Pe are defined as $El = Wi/Re$ and $Pe = VW/D$, respectively, where V is the flow velocity, and D is the diffusion coefficient, estimated to be $D = 3.02\times10^{-12}$ m^2/s, which has an inversely proportionality to the viscosity[1]. Additionally, the Dean number κ, defined by the ratio of the square root of the product of the inertia and centrifugal force to the viscous forces as $\kappa = 2\delta^{1/2}Re$, is also considered to evaluate the magnitude of secondary Dean flow in the curved serpentine channel, where δ is the radius ratio determined by $\delta = 4W/(D+d)$. The Prandtl number Pr is defined by $Pr = \nu/\alpha$, where α is the fluid thermal diffusivity defined as $\alpha = k/(\rho c_p)$, where k is the thermal conductivity coefficient and c_p is the specific heat.

Table 1 Fluid properties.

Fluid	Density ρ ($\times10^3$ kg/m^3)	Longest relaxation time λ (s)
WATER	0.995	_
25PAAM	0.995	0.067
50PAAM	0.995	0.101

Table 2 Ranges of the dimensionless parameters

Abb.	Dimensionless numbers	Expression	Definition	Range (or Value)
Re	Reynolds	$\rho UW/\eta$	Inertia / Viscous	0.15 – 0.48
Wi	Weissenberg	$\lambda\dot{\gamma}$	Polymer relaxation time / Shear rate time	3.90 – 10.10
El	Elastic	Wi/Re	Elastic / Inertia	21.31-26.90

Pe	Peclet	*VW*/*D*	Convective / Diffusive	19.40×10^{6}-33.30×10^{6}
κ	Dean	$2\delta^{1/2}Re$	The ratio of the square root of the product of the inertia and centrifugal force to the viscous force	0.75×10^{-2}-2.45×10^{-2}
Pr	Prandtl	ν/α	Viscous / Thermal	1.47-2.80

Results and Discussion

Dye pattern. The investigation was conducted when the stable flow patterns formed after the main and dye streams of fluids were injected to the serpentine channel. The dye spreading patterns are observed far downstream in the visualized region (as shown in Fig. 1(a)) from the third section to the sixth section. Fig. 1(b) and (c) show space time dye patterns of Newtonian fluids and shear-thinning fluids at a bulk flowrate $V_b = 3500$ μl/min, respectively. For the Newtonian fluid, the profile shows typical laminar dye layer with minimal dye penetration into the undyed stream, except for the weak molecular diffusion effect. However when the Newtonian fluid is replaced by the shear-thinning fluid under the same experimental condition, as shown in Fig. 1 (c), irregular flow patterns with spikes of dye were penetrated into the undyed fluid stream, showing an enhanced mixing effect.

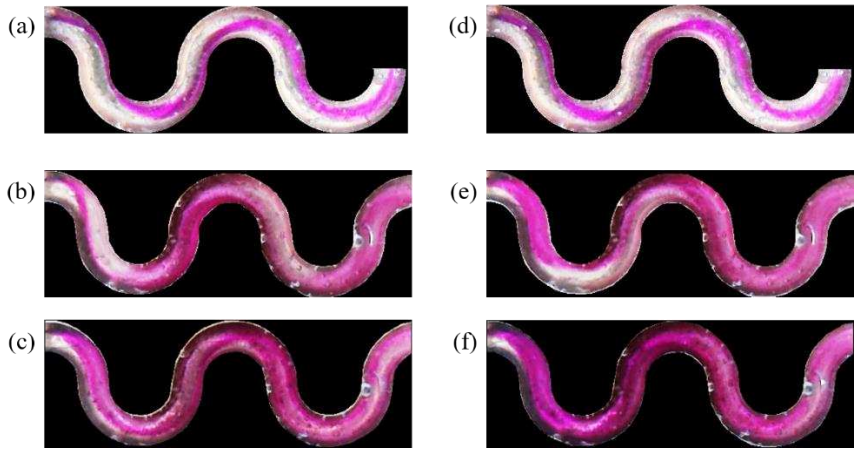

Fig. 4 Flow visualization images (a) (b) (c) WATER, 25PAAMM and 50PAAM at a bulk flowrate of $V_b = 3500$ ul/min (d) (e) (f) WATER, 25PPM and 50PPM at a bulk flowrate of $V_b = 5500$ ul/min.

Flow visualization of WATER, 25PAAM and 50PAAM at $V_b = 3500$ ul and $V_b = 5500$ ul, respectively,

have been presented in Fig. 4. For cases of the Newtonian fluid, the dye streams are narrow with little distortion and the flow condition maintains laminar with insignificant mixing, dominated by molecular diffusion only. The interface between the main and dye streams is smooth, stable, and well defined with no penetration, overlapping, swinging, or encapsulating, as shown in Fig. 4 (a) and (d). With increased flowrates, the dye stream slightly moves down from the upper to the lower border with only minimal steady secondary flows presented accompanied by very little augmented mixing and slight movement of the flow direction in the central plane away from the center of curvature. The Newtonian fluid has negligible elasticity, and extremely low Reynolds number, so the corresponding elastic and inertial effects are insignificant while the viscous effects and the centrifugal effects play a dominant role in the flow. When that the aspect ratio is approximately near unity, an increase of velocity in the outer half of the bend and a decrease in the inner is induced in the curved channel. The orthogonal injection has strongly magnified the velocity difference between the inner and outer half of the curvature, which is responsible for the slight move of the dye trajectories. The mean shear stress is skewing by a transverse pressure gradient caused by the channel planform configuration of the orthogonal injection from the outer side[47]. Traditionally, in the channel flow with curvatures, the secondary flow is induced by inertia centrifugal effects, which is strongly influenced by the Dean number[48,49] and moderately by the radius ratio δ. In other word, Dean number indicates the intensity of the secondary flow. However, in this study, the Dean number is still not large enough to generate a Dean vortex in the cross section of the serpentine channel as shown by the visualization results of deionized water. Therefore, one can find that the secondary flow is too weak to induce the following strong instabilities in the polymeric solutions.

However, for the case of shear-thinning fluids, which are 25PAAM (as shown in Fig. 4 (b) and (e)) and 50 PAAM (as shown in Fig. 4 (c) and (f)), respectively, the mixing and flow behavior are dramatically different

from those of the Newtonian fluid. At the upstream of the channel, the moderate swinging, very weak agitation and oscillation with small amplitudes and low frequencies are observed due to the interaction of the enhanced elastic stress and the skewing secondary flow induced by the orthogonal injection. At the downstream, significant and continuous mixing is observed especially in the serpentine channel accompanied by significant oscillation, salient penetration and intermittent overlapping between the two streams, which are the remarkable characteristics of elastic instability. Such elastic stress gradient leads to initial polymer distortion and agitation, and increased unstable polymer stretching at both the circumferential and normal direction due to the long relaxation time of the long-chain polymers. This significant and sharp mixing within the four bends indicates a very short mixing path within the polymeric flow. The shortened mixing path is ascribed to two factors. First, the balance between the centrifugal force and the normal elastic force leads to the significant oscillation of normal velocity component at the normal direction, resulting in elastic instability related to the enhancement of mixing performance. When the *Wi* exceeds the critical Weissenberg number, a small finite-size perturbation caused by such oscillation could induce a secondary flow as analyzed theoretically by Morozov and Saarloos[50], who claimed that the nonlinear subcritical instability comparing with the induction of Hopf bifurcation is an inherent characteristic in such flow of polymeric solutions. In such Hopf bifurcation, elasto-inertial traveling wave solutions which is corresponding to the transition from the linear to non-linear instability will be created from a laminar state in a pipe/channel flow of viscoelastic fluids which has been theoretically proved its existence recently by Garg et al. [51]. Second, the strong shear-thinning effect exists in the polymeric flow, which is benefit for the induction of bifurcation instability and chaotic flow in the working fluid with extremely low polymer concentration. The polymeric solutions with moderate shear-thinning occurs elastic instability beyond the critical Weissenberg number due to the important normal stress

gradient existing near the wall. This elasticity significantly enhance the shear rate at the wall and homogenizes the viscosity profiles which leading to a perfect mixing as reported by Bodiguel et al. [52]. In regard to the secondary flow, the coupling of analogous Dean vortices and the shear-thinning effects in the viscoelastic flows cause the augment of mixing performance since that in the viscoelastic flows, the analogous viscoelastic secondary flow can be generated even at lower Dean numbers, as presented by Poole and his co-workers[53–55] in a serpentine channel.

With higher polymer concentrations and flowrates, the valid mixing is induced earlier in the channel. This result indicates that the enhanced polymer concentration contributes to the effective mixing due to the enhanced elastic instability by the incremental non-linear elastic stress gradient, originated from the stronger polymer stretching, roiling, twining and spiraling in dilute polymer solutions.

The phenomenon unexpected here is that, at the fourth semi-section, dyed streams in the flow of water tend to be closer to the upper border while that of the viscoelastic fluid tend to be closer to the lower one at the corresponding section. The trend direction of the viscoelastic fluids is opposite to that of the centrifugal force. This unique, anti-physical and unstable phenomenon might be originated from the interaction of the curvature of the serpentine channel with the significant first normal stress difference existing in the flow of polymeric fluids. The enhanced normal stress beyond the centrifugal force in the polymeric solutions tends to stretch the polymer inside and cause this inverse behavior.

Probability density function. Quantitative mixing performance is evaluated using the probability density function (PDF) of the intensity images normalized by its overall average value, which is resemble to the method used by Gan et al.[1]. The magnitude of mixing is evaluated by the PDFs of the normalized dye concentrations based on the image sequences. During each experimental group, a data sequence including

more than 8000 data points is obtained with a time interval of 30 fps (frames per second). And then the data is statistically analyzed using the discrete distribution of the normalized concentrations over the ROI area of the channel by splitting the range from 0 to 1 to more than 50 bins equally. In this condition, a function with two respective peaks at the low and high normalized concentrations means that the fluids of the main stream and the dye stream are not mixed effectively, while a smooth PDF gathered in the middle range with nearly one peak indicates that the two streams are entirely mixed by the induced chaotic flow. Fig. 5 shows the PDFs of the flows of shear-thinning fluids and Newtonian fluid within the ROI regime (i.e., region of interest, which refers to the fourth dyed bend as shown in Fig. 4) at the flow rate of V_b=5000 ul/min. The PDF of WATER has two significant lathy peaks at the extremely low concentration and near the highest concentration, indicating deficient mixing while that of 25PAAM or 50PAAM has a negligible peak at low concentrations and a significant platform peaking in the mid-range which indicates effective mixing. In comparison with 25PAAM, the median of 50PAAM is much closer to the perfect mixing since the increased polymer concentration causing elastic stress enhancement. Therefore, effective mixing was achieved in shear-thinning fluids with extremely low concentrations which has a very low Reynolds number and a very large Peclet number.

After normalization of the dye intensity ranging from 0 to 1, the mixing efficiency σ can be quantified based on the following function. The mixing efficiency σ is defined quantitatively as follows with the normalized concentration of dye intensity ranging from 0 to 1[1]:

$$\sigma=\left[1-\frac{\sum_{i=0}^{i=1}|C_i-C_\infty|P(C_i)}{C_\infty}\right]\%$$

where C_i is the observed concentration normalized, C_∞ is the concentration normalized for fully mixing, and $P(C_i)$ is the probability density. In our study, C_∞ is estimated to be 0.4 for perfect mixing by calculating

the average normalized concentration of the completely mixed regimes. With this definition, $\sigma = 0$ means no mixing while $\sigma = 1$ means fully mixing. Thus, the mixing efficiency σ was found to be 0.21 in the flow of WATER and 0.69 and 0.76 in the flow of 25PAAM and 50PAAM, indicating that the addition of small amount of polymer only dissolving into the Newtonian fluids has significantly improved the mixing performance.

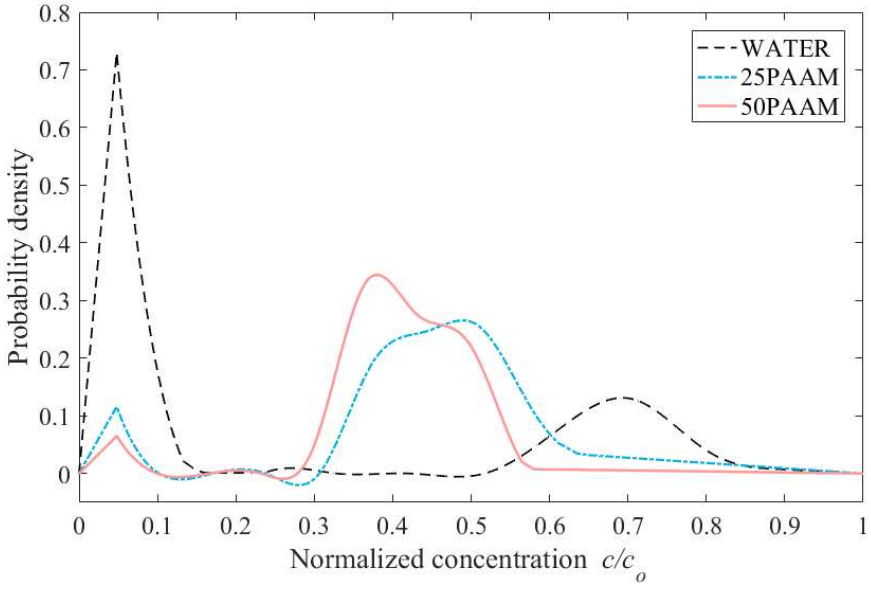

Fig. 5 Probability density function (PDF) of normalized concentration of the dye within the ROI area of the channel of WATER, 25PAAM and 50PAAM, respectively, at the flowrate of V_b=5000ul / min.

Power spectrum. Power spectra shows the power law behavior of a flow. The power-law exponent is a quantitative way to characterize the existence of the chaotic flow motion. For example, the lower absolute power-law exponent keeping constant means that the main stream and the dye stream are not mixed and the instability and chaotic flow are not induced. A high power-law exponent higher than 3 means effective mixing and inducement of chaotic flow. The fluctuation of normalized concentration is nonperiodic and obviously has power law decay, which indicates that the mixing is induced in various time scales. In this study, the Power Spectra Distribution (PSD) of the time series of fluctuations of normalized concentration is calculated by the

Fast-Flourier Transform (FFT) method in MATLAB based on 8000 data points. As shown in Fig. 6 (a), the power-law exponent of the shear-thinning solutions is approximately 3.4. The spectra do not exhibit remarkable peaks and have broad region of power law decay, which is typical for turbulent flow[27]. We observed that the power law decay is dependent on the flowrates and has non-monotonic behavior. Such decay has been interpreted as the evidence of elastic turbulence. In comparison, for the case of Newtonian fluids, the power spectrum is extremely flat corresponding with noise. We believe that such chaotic flow leads to the enhanced effective mixing due to the enhancement of non-linear elastic stress gradient. The absolute power-law exponent of Newtonian fluids stays around 2, closely related to the laminar flow as illustrated in Fig. 6 (b). Adversely, the absolute power-law exponent of polymeric solutions gradually increases with the bulk flowrates and reaches a platform at 3.4 at the value of V_b around 4000 μl and 6000 μl for 25PAAM and 50PAAM, respectively, which indicates that the flow is fully chaotic. This saturated exponent is independent on the polymer concentration and have been investigated in our previous studies [42]. When the polymer solutions are normalized by the relaxation time, the transition point of the fully chaotic regime are similar around Wi=6.7 for both concentrations as shown in Fig. 6. In this present work, the differences of polymer contribution to the viscosity between those polymer solutions are insignificant due to the much dilute concentration. Therefore, the critical Wi is in same level for both polymer solutions. In addition, the absolute power-law exponent plateaus more quickly at a lower flowrate in the polymeric solution with a slightly higher polymer concentration. The changes in the exponent observed here can be explained by the different driving mechanisms of the processes of mixing, of which the Newtonian fluid is molecular diffusion purely and the shear-thinning fluid is driven by the induced chaotic flow. The dramatically growth of the absolute exponent proves that the flow condition transferring from laminar to elastic instability. We believe that the slightly more

polymer addition into the Newtonian fluids leads to the stronger polymer stretching, resulting in the enhancement of normal elastic stress gradient and the corresponding non-linear flow instability[14]. The power law spectra of the normalized concentration show a high frequency oscillation. Contrary to general case, where the power-law decay of the normalized concentration corresponding to elastic turbulence commences at f = -1, the mixing in such orthogonal flows cause the power-law spectra start to decay at lower frequencies as shown in the figure, perhaps due to the high frequency oscillations.

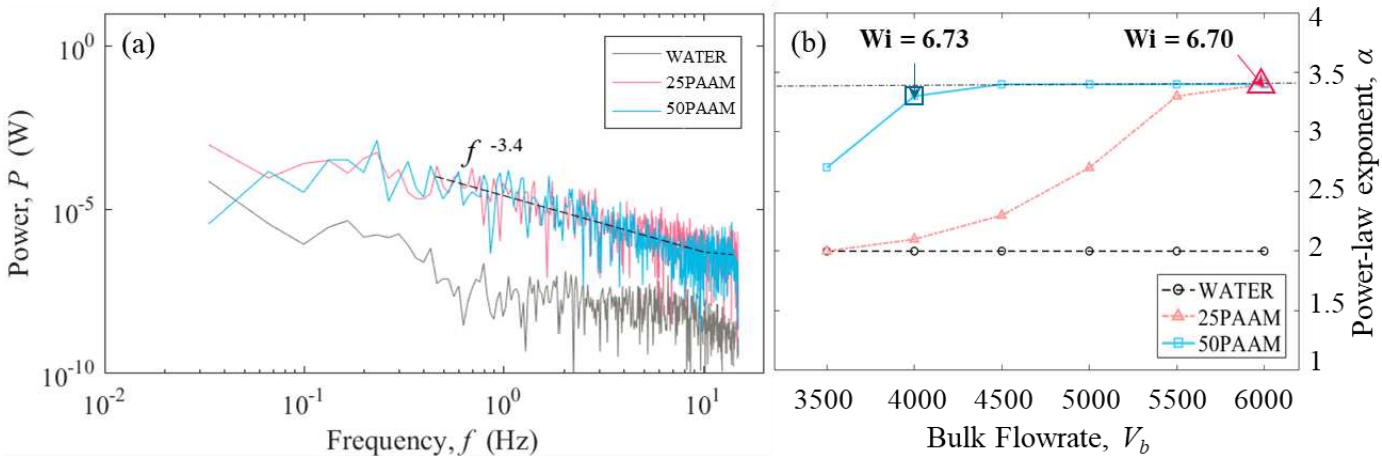

Fig. 6 Power spectra of the total normalized concentration in the dyed area at the flowrate V_b = 5000 µl/min (b) Absolute power-law exponent versus flowrates from V_b = 3500 µl/min to V_b = 6000 µl/min.

Fluctuations. The increase in mixing is closely associated with the onset of fluctuations of the relative change ratio of the total normalized concentration (Fig. 7) which is defined as follows:

$$\gamma(i)=\frac{I_{i+1}-I_i}{I_i}\times 100\%$$

where I_i is the relative change ratio of the total normalized concentration in the dyed area, i is the series of images captured by a frequency of 30Hz, which has been reported as a suitable frequency to capture the flow characteristics of elastic instability and elastic turbulence[56]. We observe a clear increase in the fluctuations of the relative change ratio of the total normalized concentration in the dyed area. Fig. 7 (a) shows the evolution

of such fluctuations within the sampling time. We illustrate the time dependent flow by showing a series of dye advection images in Fig. 8 (a)-(c). In the flow of polymeric solutions, the interfaces between the dyed and undyed fluids becomes unclear and oscillates with time, while in the flow of Newtonian fluids, the interface is sharp and steady. This indicates that a three-dimensional chaotic flow is induced here and becomes very complex which is comparable with the phenomenon shown by Arratia et al.[57] in the flow within a cross-channel flow.

Fig. 8(d) shows root-mean-square (rms) values of the relative-change-ratio fluctuations of both Newtonian and two shear-thinning fluids, respectively, as a function of flowrates. For the Newtonian fluid, the relative-change-ratio fluctuation remains small and steady, nearly independent of flowrate; the negligibly small increase in the fluctuation may be due to insignificant molecular diffusion. For polymer solutions, the rms values significant departure from the stable case of none polymer additions and shows a remarkable enhancement with increased flowrates companied by more irregular, more frequent, and stronger fluctuations until the secondary flow looks fully turbulent-like[58]. With the increase of polymer concentrations, the values of rms separate and plateau earlier at a lower flowrate which indicates that the transitions from laminar to subcritical instability and to chaotic flows with significant bifurcation instability occurs earlier, respectively. The amplitude of the fluctuation is not very large, and the signal jumps from the low dye rate to the high one frequently which is strongly benefit for the achievement of effective mixing as illustrated in Fig. 8. These results strongly indicate that a time-dependent flow can be created and sustained even with a very small amount of polymer addition when the flowrates exceeding a critical number. The relative-change-ratio of the concentrations is strongly fluctuating and its time dependence has well expressed chaotic advections. The chaotic performance is confirmed by the analysis of the root-mean-square (rms) of the relative-change-ratio

of the concentrations. These trends agree relatively well with the relative-change-ratio fluctuations and the bifurcation instability observed in the flow visualization. Since that now the fluctuation of the relative-change-ratio of the concentrations from the dyed space-time patterns (as examples in Fig. 4 shows) is available, it is convenient to investigate the rule of flow state transitions for viscoelastic channel flows from the rms development. Traditionally, for Newtonian fluids, the rms keeps small with negligible variations and independent on the Weissenberg number. In what follows for polymeric solutions, we proposed that the rms relative-change-ratio fluctuations is a good method to quantitatively scales the degree of elastic instability and the transition from linear instability to a bifurcation instability and corresponding mixing performance.

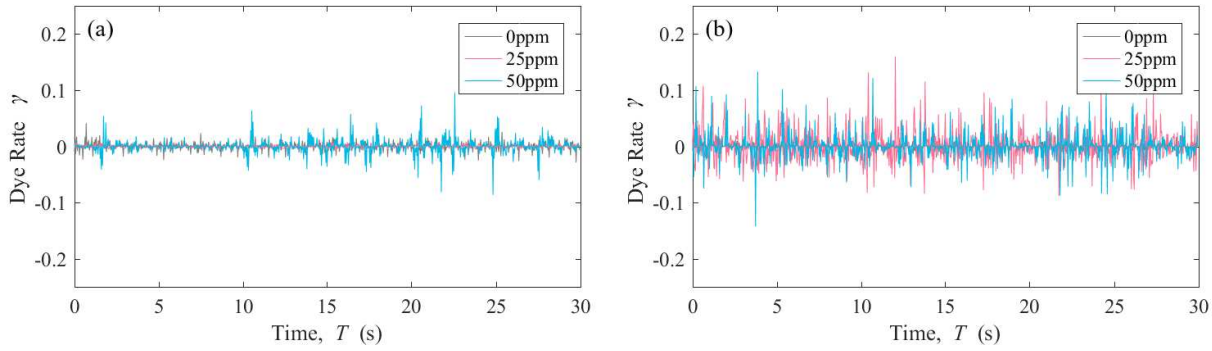

Fig. 7 Fluctuations of the relative change ratio of the total normalized concentration of the dyed area versus time with solutions of Water, 25PAAM and 50PAAM, respectively. (a) At the flowrate V_b = 3500 μl/min. (b) At the flowrate V_b = 5000 μl/min.

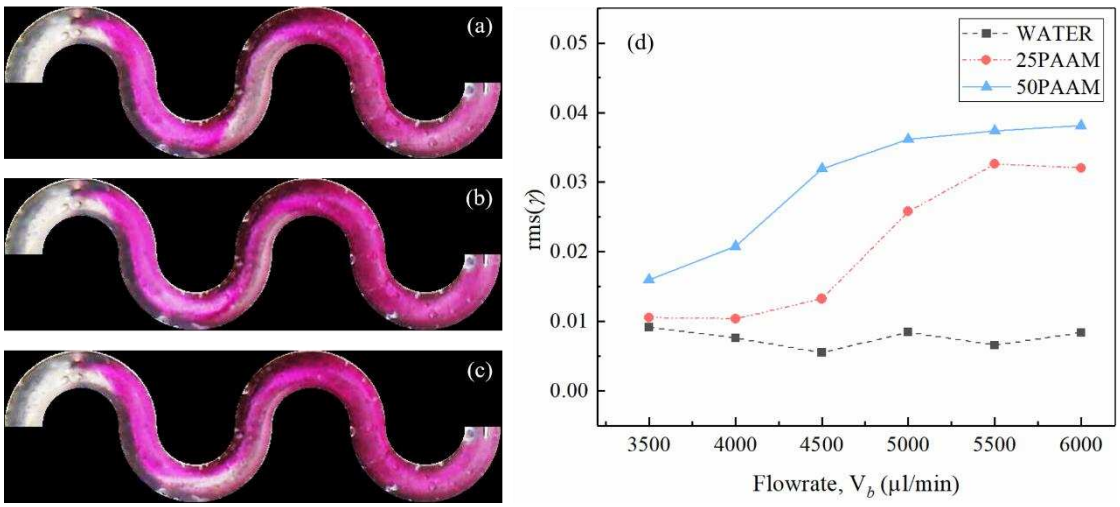

Fig. 8 (a)-(c) Dye advection patterns for the polymer solution with the concentration of 25 ppm in the time dependent regime

(V_b = 6000 μl/min) at 3s intervals. (d) Root-mean-square (rms) of the fluctuations of the relative change ratio of the total normalized concentration of the dyed area as a function of flowrate for WATER, 25PAAM and 50PAAM.

Conclusion. In summary, a novel and effective micro mixer with orthogonal injection in the serpentine channel is proposed in this study. We have compared mixing behavior between the Newtonian fluid and shear-thinning fluids with low polymer concentrations in a micro serpentine channel with negligible inertial effect (low Re), and demonstrated that the orthogonal injection could boost the induction of elastic instability and promote effective mixing due to the augment of the interaction between the first normal stress difference and curvatures. A much earlier induced elastic instability is observed along the serpentine channel. Effective mixing is induced by the unstable chaotic flow via a nonlinear subcritical instability for finite perturbations. Even extremely small perturbations generated from the increased normal elastic stress gradient in the flow have the capability to induce significant mixing. The following conclusions can be drawn:

1. The progress of effective mixing and flow trajectories are developed over a short distance within the micro serpentine channel as proved by the dye visualization. Based on the new method, the main and dye streams of fluids can be easily mixed at a very short mixing length by using shear-thinning fluids with extremely low polymer concentrations. With the increase of flowrate and polymer concentration, flow instability transits from weak bifurcation instabilities to dramatically chaotic turbulence.
2. Effective mixing with a short mixing path is quantitatively characterized by statistical analysis. Probability Density Function (PDF) of normalized dye concentrations of the fluids indicates that the mixing efficiency can be significantly increased from 22% for the Newtonian fluids to 69% and 76% for the 25 and 50 PAAM respectively. The decay exponents of shear-thinning fluids plateau at -3.4 indicates the onset of elastic instability and chaotic flow. The relative-change-ratio fluctuations illustrated in the

observation area can generate sufficient normal elastic stress gradients to sustain the flow instabilities, resulting in effective mixing in the channel flow.

Our results show strong evidence for the "instability upon an instability" mechanism mentioned by Qin et al.[40] and provide a new method and device for the simplest mixing enhancement in micro channels without plenty of additions. We prove experimentally that the orthogonal injection is beneficial to achieve efficient mixing within a shorted mixing path. This work, provide a simple approach, by exploiting viscoelastic flow instability affected by shear-thinning effects, to enhance mixing in micro channels over a very short distance. Further studies are being undertaken to establish the velocity fields by using micro-PIV.

Acknowledgements. The authors would like to thank the NSFC (National Natural Science Foundation of China) for its financial supports (Grants 51876006) and the support from Beijing Municipal Science and Technology Commission.

Reference

[1] H.Y. Gan, Y.C. Lam, N.T. Nguyen, K.C. Tam, C. Yang, Efficient mixing of viscoelastic fluids in a microchannel at low Reynolds number, Microfluid. Nanofluid. 3 (2007) 101–108.

[2] D. Yuan, Q. Zhao, S. Yan, S.-Y. Tang, G. Alici, J. Zhang, W. Li, Recent progress of particle migration in viscoelastic fluids, Lab Chip. 18 (2018) 551–567.

[3] I. Mezić, S. Loire, V.A. Fonoberov, P. Hogan, A new mixing diagnostic and Gulf oil spill movement, Science. 330 (2010) 486–489.

[4] Hartman, R. L.; Jensen, K. F. Microchemical Systems for Continuous-Flow Synthesis. *Lab Chip* **2009**, *9* (17), 2495–2507.

[5] Park, J. I.; Saffari, A.; Kumar, S.; Günther, A.; Kumacheva, E. Microfluidic Synthesis of Polymer and Inorganic

Particulate Materials. *Annu. Rev. Mater. Res.* **2010**, *40* (1), 415–443.

[6] T. Frommelt, M. Kostur, M. Wenzel-Schäfer, P. Talkner, P. Hänggi, A. Wixforth, Microfluidic Mixing via Acoustically Driven Chaotic Advection, Phys. Rev. Lett. 100 (2008) 034502.

[7] K.L. Helton, P. Yager, Interfacial instabilities affect microfluidic extraction of small molecules from non-Newtonian fluids, Lab Chip. 7 (2007) 1581–1588.

[8] V. VanDelinder, A. Groisman, Separation of plasma from whole human blood in a continuous cross-flow in a molded microfluidic device, Anal. Chem. 78 (2006) 3765–3771.

[9] S.O. Hong, J.J. Cooper-White, J.M. Kim, Inertio-elastic mixing in a straight microchannel with side wells, Appl. Phys. Lett. 108 (2016) 014103.

[10] T.J. Johnson, D. Ross, L.E. Locascio, Rapid Microfluidic Mixing, Anal. Chem. 74 (2002) 45–51.

[11] A. Alam, K.-Y. Kim, Analysis of mixing in a curved microchannel with rectangular grooves, Chem. Eng. J. 181–182 (2012) 708–716.

[12] L.-M. Fu, W.-J. Ju, C.-H. Tsai, H.-H. Hou, R.-J. Yang, Y.-N. Wang, Chaotic vortex micromixer utilizing gas pressure driving force, Chem. Eng. J. 214 (2013) 1–7.

[13] J.M. Ottino, APPLIED PHYSICS: Designing Optimal Micromixers, Science. 305 (2004) 485–486.

[14] Anupam Gupta1 and Dario Vincenzi, Effect of polymer-stress diffusion in the numerical simulation of elastic turbulence, J. Fluid Mech. 870 (2019) 405–418.

[15] S. Belan, A. Chernykh, V. Lebedev, Boundary layer of elastic turbulence, J. Fluid Mech. 855 (2018) 910–921.

[16] A. Groisman, V. Steinberg, Elastic turbulence in a polymer solution flow, Nature. 405 (2000) 53.

[17] M.M. Afonso, D. Vincenzi, Nonlinear elastic polymers in random flow, J. Fluid Mech. 540 (2005) 99–108.

[18] S. Berti, G. Boffetta, Elastic waves and transition to elastic turbulence in a two-dimensional viscoelastic Kolmogorov

flow, Phys. Rev. E. 82 (2010) 036314.

[19] T. Burghelea, V. Steinberg, P.H. Diamond, Internal viscoelastic waves in a circular Couette flow of a dilute polymer solution, EPL. 60 (2002) 704.

[20] T. Burghelea, E. Segre, V. Steinberg, Role of elastic stress in statistical and scaling properties of elastic turbulence, Phys. Rev. Lett. 96 (2006) 214502.

[21] C.C. Hopkins, S.J. Haward, A.Q. Shen, Purely Elastic Fluid–Structure Interactions in Microfluidics: Implications for Mucociliary Flows, Small. 16 (2020) 1903872.

[22] M. Grilli, A. Vázquez-Quesada, M. Ellero, Transition to Turbulence and Mixing in a Viscoelastic Fluid Flowing Inside a Channel with a Periodic Array of Cylindrical Obstacles, Phys. Rev. Lett. 110 (2013) 174501.

[23] A. Varshney, V. Steinberg, Mixing layer instability and vorticity amplification in a creeping viscoelastic flow, Phys. Rev. Fluids. 3 (2018) 103303.

[24] T. Burghelea, E. Segre, V. Steinberg, Mixing by Polymers: Experimental Test of Decay Regime of Mixing, Phys. Rev. Lett. 92 (2004) 164501.

[25] T. Burghelea, Chaotic flow and efficient mixing in a microchannel with a polymer solution, Phys. Rev. E. 69 (2004) 066305.

[26] Y. Jun, V. Steinberg, Mixing of passive tracers in the decay Batchelor regime of a channel flow, Phys. Fluids. 22 (2010) 123101.

[27] A. Groisman, V. Steinberg, Efficient Mixing at low Reynolds numbers using polymer additives, Nature. 410 (2001) 905–908.

[28] A. Afonso, M.A. Alves, R.J. Poole, P.J. Oliveira, F.T. Pinho, A Novel Microfluidic Mixing Element for Viscoelastic Fluids, AIP Conference Proceedings. 1027 (2008) 1009–1011.

[29] A.M. Afonso, M.A. Alves, R.J. Poole, P.J. Oliveira, F.T. Pinho, Viscoelastic flows in mixing-separating cells, J. Eng. Math. 71 (2011) 3–13.

[30] C.A. Browne, A. Shih, S.S. Datta, Pore-Scale Flow Characterization of Polymer Solutions in Microfluidic Porous Media, Small. 16 (2020) 1903944.

[31] A. Zizzari, M. Cesaria, M. Bianco, L.L. del Mercato, M. Carraro, M. Bonchio, R. Rella, V. Arima, Mixing enhancement induced by viscoelastic micromotors in microfluidic platforms, Chem. Eng. J. (2019) 123572.

[32] H.Y. Gan, Y.C. Lam, N.-T. Nguyen, Polymer-based device for efficient mixing of viscoelastic fluids, Appl. Phys. Lett. 88 (2006) 224103.

[33] P. Ligrani, D. Copeland, C. Ren, M. Su, M. Suzuki, Heat Transfer Enhancements from Elastic Turbulence Using Sucrose-Based Polymer Solutions, J. Thermophys. Heat Transf. 32 (2018) 51–60.

[34] P.M. Ligrani, M. Su, A. Pippert, R.A. Handler, Thermal Transport of Viscoelastic Fluids Within Rotating Couette Flows, J. Thermophys. Heat Transf. 34 (2020) 121–133.

[35] S.J. Haward, C.C. Hopkins, A.Q. Shen, Asymmetric flow of polymer solutions around microfluidic cylinders: Interaction between shear-thinning and viscoelasticity, Journal of Non-Newtonian Fluid Mechanics. 278 (2020) 104250.

[36] M.P. Escudier, A.K. Nickson, R.J. Poole, Turbulent flow of viscoelastic shear-thinning liquids through a rectangular duct: Quantification of turbulence anisotropy, J. Non-Newton. Fluid Mech. 160 (2009) 2–10.

[37] L. Casanellas, M.A. Alves, R.J. Poole, S. Lerouge, A. Lindner, The stabilizing effect of shear thinning on the onset of purely elastic instabilities in serpentine microflows, Soft Matter. 12 (2016) 6167–6175.

[38] V. Kantsler, V. Steinberg, Transition to tumbling and two regimes of tumbling motion of a vesicle in shear flow, Phys. Rev. Lett. 96 (2006) 036001.

[39] M.P. Escudier, R.J. Poole, F. Presti, C. Dales, C. Nouar, C. Desaubry, L. Graham, L. Pullum, Observations of

asymmetrical flow behaviour in transitional pipe flow of yield-stress and other shear-thinning liquids, J. Non-Newton. Fluid Mech. 127 (2005) 143–155.

[40] B. Qin, P.F. Salipante, S.D. Hudson, P.E. Arratia, Flow Resistance and Structures in Viscoelastic Channel Flows at Low Re, Phys. Rev. Lett. 123 (2019) 194501.

[41] R.M. Bryce, M.R. Freeman, Abatement of mixing in shear-free elongationally unstable viscoelastic microflows, Lab Chip. 10 (2010) 1436–1441.

[42] G. Yao, J. Zhao, H. Yang, D. Wen, Effects of salinity on the onset of elastic turbulence in swirling flow and curvilinear microchannels, Phys. Fluids. 31 (2019) 123106.

[43] P. Ligrani, B. Lund, A. Fatemi, Miniature Viscous Disk Pump: Performance Variations From Non-Newtonian Elastic Turbulence, J. Fluids Eng. 139 (2017) 021104.

[44] H. Yang, G. Yao, D. Wen, Experimental investigation on convective heat transfer of Shear-thinning fluids by elastic turbulence in a serpentine channel, Experimental Thermal and Fluid Science. 112 (2020) 109997.

[45] R.A. Handler, E. Blaisten-Barojas, P.M. Ligrani, P. Dong, M. Paige, Vortex generation in a finitely extensible nonlinear elastic Peterlin fluid initially at rest, Engineering Reports. 2 (2020) 12135.

[46] R.B. Bird, ed., Dynamics of polymeric liquids: Fluid mechanics, 2nd ed, Wiley, New York, 1987.

[47] Q. Zhao, D. Yuan, J. Zhang, W. Li, A Review of Secondary Flow in Inertial Microfluidics, Micromachines. 11 (2020) 461.

[48] P.M. Ligrani, R.D. Niver, Flow visualization of Dean vortices in a curved channel with 40 to 1 aspect ratio, Physics of Fluids. 31 (1988) 3605.

[49] P.M. Ligrani, C.R. Hedlund, Experimental Surface Heat Transfer and Flow Structure in a Curved Channel With Laminar, Transitional, and Turbulent Flows, J. Turbomach. 126 (2004) 414–423.

[50] A.N. Morozov, W. van Saarloos, Subcritical Finite-Amplitude Solutions for Plane Couette Flow of Viscoelastic Fluids, Phys. Rev. Lett. 95 (2005) 024501.

[51] P. Garg, Viscoelastic Pipe Flow is Linearly Unstable, Phys. Rev. Lett. 121 (2018) 024502.

[52] H. Bodiguel, J. Beaumont, A. Machado, L. Martinie, H. Kellay, A. Colin, Flow enhancement due to elastic turbulence in channel flows of shear thinning fluids, Phys. Rev. Lett. 114 (2015) 028302.

[53] L. Ducloué, L. Casanellas, S.J. Haward, R.J. Poole, M.A. Alves, S. Lerouge, A.Q. Shen, A. Lindner, Secondary flows of viscoelastic fluids in serpentine microchannels, Microfluid. Nanofluid. 23 (2019) 33.

[54] L. Toribio, S. Arranz, A.M. Ares, J. Bernal, Polymeric stationary phases based on poly (butylene terephthalate) and poly (4-vinylpirydine) in the analysis of polyphenols using supercritical fluid chromatography. Application to bee pollen, Journal of Chromatography A. 1572 (2018) 128–136.

[55] M. Davoodi, S. Lerouge, M. Norouzi, R.J. Poole, Secondary flows due to finite aspect ratio in inertialess viscoelastic Taylor–Couette flow, J. Fluid Mech. 857 (2018) 823–850.

[56] A. Varshney, V. Steinberg, Elastic Alfven waves in elastic turbulence, Nat. Commun. 10 (2019) 652.

[57] P.E. Arratia, C.C. Thomas, J. Diorio, J.P. Gollub, Elastic instabilities of polymer solutions in cross-channel flow, Phys. Rev. Lett. 96 (2006) 144502.

[58] R. van Buel, C. Schaaf, H. Stark, Elastic turbulence in two-dimensional Taylor-Couette flows, EPL. 124 (2018) 14001.

[59] G.H. McKinley, P. Pakdel, A. Oztekin, Rheological and geometric scaling of purely elastic flow instabilities, J. Non-Newton. Fluid Mech. 67 (1996) 19–47.

[60] A. Groisman, V. Steinberg, Mechanism of elastic instability in Couette flow of polymer solutions: Experiment, Phys. Fluids. 10 (1998) 2451–2463.

[61] A. Groisman, V. Steinberg, Elastic turbulence in curvilinear flows of polymer solutions, New J. Phys. 6 (2004) 29.

[62] T. Burghelea, E. Segre, V. Steinberg, Elastic turbulence in von Karman swirling flow between two disks, Phys. Fluids. 19 (2007) 053104.

[63] J. Zilz, R.J. Poole, M.A. Alves, D. Bartolo, B. Levaché, A. Lindner, Geometric scaling of a purely elastic flow instability in serpentine channels, J. Fluid Mech. 712 (2012) 203–218.

[64] A. Groisman, V. Steinberg, Stretching of polymers in a random three-dimensional flow, Physical Review Letters. 86 (2001) 934.

[65] D.W. Beard, M.H. Davies, K. Walters, The stability of elastico-viscous flow between rotating cylinders Part 3. Overstability in viscous and Maxwell fluids, Journal of Fluid Mechanics. 24 (1966) 321–334.

[66] B. Qin, P.E. Arratia, Characterizing elastic turbulence in channel flows at low Reynolds number, Phys. Rev. Fluids. 2 (2017) 083302.